12870 *J. Phys. Chem. A* **2006,** *110,* 12870−12881

Hydride Affinities of Some Substituted Alkynes: Prediction by DFT Calculations and Rationalization by Triadic Formula

Robert Vianello,*,† Nena Peran,† and Zvonimir B. Maksić†,‡

Quantum Organic Chemistry Group, Division of Organic Chemistry and Biochemistry, Ruđer Bošković Institute, POB 180, 10002 Zagreb, Croatia, and Faculty of Science, University of Zagreb, Horvatovac 102A, 10000 Zagreb, Croatia

Received: July 14, 2006; In Final Form: September 15, 2006

Hydride affinities (HAs) of the ethynes substituted by a wide range of different substituents are considered by using the B3LYP methodology. The computed values are in fair agreement with available experimental data, which are unfortunately scarce. The trend of changes of the HAs is rationalized by trichotomy formula. One of the important results of this analysis is a finding that similar HA values might result from completely different effects. Alternative sites of the H^- attack are examined and the difference in energies relative to the most susceptible positions is interpreted. Structural features of substituted ethyne hydrides are briefly discussed.

Introduction

It is common knowledge that the proton is pivotal in defining Brønsted acids and bases. The proton is the simplest Lewis acid and a very hard electrophile at the same time. Almost countless scientific papers have been dedicated to the problems of proton affinity or deprotonation energy of organic, inorganic, and biological molecules. In contrast, surprisingly little attention has been devoted to its counterpart—the smallest Lewis base and the simplest nucleophile—the hydride ion H^-. This is notwithstanding with its role in chemical reactions.[1] For example, reduction of carbonyl compounds to alkoxides by the use of hydriding reagents such as $LiAlH_4$, $NaBH_4$, AlH_3, H_2/catalyst, or B_2H_6 is a key step in many chemical transformations.[1] Furthermore, intramolecular 1,2- and transannular-hydride shifts are widely used in carbocation rearrangement chemistry.[2,3] It is important to mention that intermolecular hydride transfers have long been industrially exploited.[4−6] The biochemical relevance of the hydride transfer is evidenced by acceptor coenzymes NAD^+ and $NADP^+$, which include reactions catalyzed by a number of dehydrogenases[7] and the interconversion of galactose and glucose,[8] to mention just a few of them. The experimental measurements of the hydride affinities (HAs) of some quinones, organic radicals, and cations in solvents have been reported by Parker and co-workers.[9−12] Despite these efforts the measured data are sparse,[13] which is rather unfortunate. Namely, these values could serve as a good probe of electrophilic propensity for important series of compounds. The number of theoretical treatments is not much higher either. They are usually confined to the electron charge redistribution upon hydride addition[14] or use of the isodesmic reactions in treating hydride affinities.[15] Both approaches suffer from some interpretive shortcomings. The atomic charge distribution is just one parameter, which affects the hydride in an implicit and consequently not a transparent way, apart from their arbitrary formal definition. Particularly the frequently used QTAIM[16] (quantum theory of atoms in molecule) charges[14] have some well-documented drawbacks (see later). The isodesmic reactions are able to provide correct estimates of the initial and final state contributions to the HAs,[15] but the process of hydration is much more subtle than that. A more detailed description is offered by the triadic approach, which has been successfully applied to proton affinities of neutral molecules[17] (Brønsted basicity) and anions[18] (Brønsted acidity). Triadic (trichotomy) formula has some distinct advantages over more traditional ways of rationalization of acidity and basicity trends in series of related compounds as thoroughly discussed by Deakyne in a recent review.[19] It proved also useful in explaining the substituent effects.[20] It is gratifying that the triadic paradigm can be easily extended to hydride affinities as shown in the case of borane (BH_3) derivatives recently.[21] Building on these results we consider here the HAs of some substituted ethynes, HC≡CR, where R stands for a variety of widely different substituents. The aim of this work is 2-fold: (1) to find the most susceptible positions to the H^- attack and provide reliable theoretical HAs of compounds, which were not submitted to the experimental investigations earlier, and (2) to shed more light on the underlying principles governing HAs, as revealed by triadic formula. Both aspects are of equal importance. It is essential to have at one's disposal as much data on the HAs as possible, which are interesting per se, and it is also quintessential to contribute toward their understanding. The latter is a prerequisite for designing new compounds exhibiting predetermined hydride affinities, to mention hydride sponges as an important example. In addition to the energetic considerations, we shall briefly discuss structural features of hydrides, the changes in hybridization, and redistribution of charges induced by the H^- nucleophilic attack.

Theoretical Framework and Computational Details

The gas-phase hydride affinities (HAs) are defined by the negative enthalpy change of a reaction:

$$M + H^- \rightarrow (M_\alpha H)^- - (HA)_\alpha \qquad (1)$$

where M is a molecule in its oxidized state and $(M_\alpha H)^-$ is its reduced hydrided form. The site of the H^- attack is denoted by

---

* Corresponding author. Tel: +385-1-4561117. Fax: +385-1-4561118. E-mail: vianello@spider.irb.hr.

† Ruđer Bošković Institute.

‡ University of Zagreb.

10.1021/jp064463o CCC: $33.50

α. It is convenient for interpretative purposes to resolve this process into three consecutive steps: (1) the ionization of the H^- atom, (2) the electron attachment to the studied molecule M, and (3) the formation of a new homolytic bond between two newly formed radicals $M^{\bullet-}$ and $H^{\bullet}$. They are described by the adiabatic ionization energy of the hydride ion $IE_1^{ad}(H^-)$, the first adiabatic electron affinity of a molecule in question $EA_1^{ad}(M)$, and the bond association energy $(BAE)_\alpha^{\bullet-}$ between two radicals $M^{\bullet-}$ and $H^{\bullet}$, respectively. The thermodynamical balance of reaction 1 yields

$$(HA)_\alpha = EA_1^{ad}(M) + (BAE)_\alpha^{\bullet-} - 17.4\ \mathrm{kcal\ mol^{-1}} \quad (2)$$

where 17.4 kcal mol^{-1} stands for the experimentally determined ionization energy of H^-.[22] It is important to mention that the first two terms include the zero point vibrational energy (ZPVE) contributions, which gives the "cold energy" part of the hydride affinity at $T = 0$ K. Subsequently, the system $(M_\alpha H)^-$ is warmed up to room temperature ($T = 298$ K), implying that the corresponding vibrational corrections are taken into account for both $EA_1^{ad}(M)$ and $(BAE)_\alpha^{\bullet-}$ terms. The $(5/2)RT$ additive constant is assigned to the bond association energy for obvious reasons. It is useful to delineate the inherent properties of the initial state of a molecule M under study from other interlocked effects occurring in production of the resulting anion $(M_\alpha H)^-$. It would be incorrect, however, to identify $EA_1^{ad}(M)$ with genuine initial properties of a molecule M, because the adiabatic electron attachment involves relaxation of both electron density and spatial structural parameters. To single out the initial properties one has to invoke Koopmans' theorem.[23] The latter states that the electron affinity $EA_n^{Koop}(M)$ is approximately given by the negative energy $-\epsilon_n$ of the corresponding unoccupied orbital calculated within the Hartree−Fock (HF) model. In other words, the electron attachment is considered to be a sudden event, where neither nuclei nor electrons are allowed to relax. Despite the roughly approximate nature of Koopmans' clamped nuclei and frozen electron picture, the calculated $EA_n^{Koop}(M)$ values are very useful when applied to families of closely related molecules.[24] It is noteworthy that $EA_n^{Koop}(M)$ does not necessarily correspond to the first electron affinity ($n = 1$), because the empty MO associated with accommodation of the excess negative charge in the electron capture event might be higher in energy than the LUMO. This important detail deserves a comment. First, it is easy to identify the MO in question, since it is the one which plays a pivotal role in the forthcoming formation of a new $(M_\alpha H)^-$ bond. For that reason we shall term it the principal molecular orbital (PRIMO). Second, if an additional electron is placed in a virtual (LUMO + m) orbital, where m is a positive natural number $m = n - 1$, the corresponding electron configuration might be unbound. However, even in this case the present approach retains its interpretive value in a formal sense, if employed within a family of closely related molecules. Finally, it should be stressed that the electron attachment is not instantaneous. It occurs in real time involving relaxation of the electrons and nuclei in the $M^{\bullet-}$ anion, which is determined by the reorganization energy defined by

$$E(ea)^{(n)}_{rex} = EA_1^{ad}(M) - EA_n^{Koop}(M) \quad (3)$$

where "ea" within parentheses denotes the electron attachment. It should be noticed that relaxation yields an interplay between the initial and final state effects, being an intermediate step on its own. Hence, the resulting triadic formula for addition of H^- ion to the molecule M, yielding the accompanying hydride affinity, is of the form

$$(HA)_\alpha = EA_n^{Koop}(M) + E(ea)^{(n)}_{rex} + (BAE)_\alpha^{\bullet-} - 17.4\ \mathrm{kcal\ mol^{-1}} \quad (4)$$

As a good compromise between the feasibility of the method and accuracy on one side and feasibility combined with economy (in terms of the computer time) on the other, we employed the B3LYP/6-311+G(2df,p)//B3LYP/6-31G(d) method. Geometry optimizations, verification of the minima on the Born−Oppenheimer potential energy hypersurface, and calculation of the thermodynamical parameters corresponding to room temperature (298.15 K) are performed at the efficient B3LYP/6-31G(d) level. Koopmans' electron affinities are obtained by the HF/6-311G(2df,p)//B3LYP/6-31G(d) model. Radical anions were treated by the unrestricted formalism at the UB3LYP/6-311+G-(2df,p)//UB3LYP/6-31G(d) level. It should be pointed out that for reliable unrestricted calculations for the open shells it is required that the expectation values of the S^2 operator is around 0.75.[25] This condition was satisfied for all radicals considered in the present paper. All computations were performed using the GAUSSIAN 98 program.[26]

Results and Discussion

Hydride Affinities. Ethyne and its derivatives encompassing CH_3, C_2H_5, C_3H_7, CN, NO_2, F, NH_2, OH, and CF_3 substituents (exhibiting widely different electron releasing or accepting properties) are examined. In addition, allene is considered, too, since its hydride is a planar system. The first problem to be addressed is the site most susceptible to the hydride ion attack. It appears that the H^- anion prefers the unsubstituted C^2 position with only one exception. The latter is given by the OH group, which makes C^1 carbon more prone to H^- attachment. The difference $HA(OH)_2 - HA(OH)_1$ is, however, very small, being 0.8 kcal mol^{-1} (Table 1). On the other hand, discrimination between C^1 and C^2 ethyne sites could be sometimes as large as 10 kcal mol^{-1} as in the case of CN and NO_2 substituents. The largest difference is found in **2**, being 17.8 kcal mol^{-1}, since hydridation at the terminal carbon destroys the anionic resonance occurring in the planar allyl system.

Perusal of the data displayed in Table 1 reveals that substituents strongly influence hydride affinity as reflected in a wide range of values placed between 37 and 100 kcal/mol. The alkyl groups practically do not affect the HA of ethyne due to their weak electron donor nature. All other electron withdrawing substituents increase hydride affinity as intuitively expected. The largest amplifying effect is exerted by the NO_2 group, to be followed by the CN and CF_3 substituents, which is in agreement with their electron accepting power. Obviously, the latter determines the electrophilic propensity of substituted alkynes in agreement with chemical intuition. Modest influence of the alkyl groups in affecting the HAs is reflected in disubstituted propynes **1k**, **1l**, **1m**, and **1n**, substituted at the other sp^1 carbon atom by F, CN, NO_2, and CF_3 groups, respectively. The HA values are fairly close to those of ethynes monosubstituted by the corresponding electronegative groups (vide infra). The H^- anion is attached to the $C(sp^1)$ atom substituted by the CH_3 group as the energetically advantageous site in the disubstituted derivatives.

The experimental data are unfortunately sparse. Theoretical results are within the experimental error bars for CH_3 and CN derivatives. The same holds for allene. In contrast, the difference

TABLE 1: Hydride Affinities of Substituted Ethynes $R^1C^1{\equiv}C^2R^2$, Relative Stabilities of Hydrides Obtained by the H^- Attack against the Parent Molecule, and Resolution of the Calculated Hydride Affinities into Triadic Components (in kcal mol^{-1})[a]

R^1	R^2	molecule	EA_n^{Koop}	EA_1^{ad}	$E(ea)^{(n)}_{rex}$	$(BAE)^{\bullet-}$	HA(thr)	ΔHA
H	H	**1a**	$(-120.7)_3$	−26.2	94.5	81.6	38.0 (34.1)	0.0
CH_3	H	**1b**^{2}	$(-121.4)_3$	−29.0	92.5	83.2	36.8 (34.4 ± 2.2)	−1.2
		1b^1	$(-121.4)_3$	−29.0	92.5	81.6	35.2	−2.8
C_2H_5	H	**1c**^{2}	$(-120.6)_3$	−27.2	93.4	83.3	38.7	0.7
		1c^1	$(-120.6)_3$	−27.2	93.4	79.4	34.9	−3.1
C_3H_7	H	**1d**^{2}	$(-117.1)_3$	−27.1	90.0	83.4	38.9	0.9
		1d^1	$(-117.1)_3$	−27.1	90.0	79.7	35.2	−2.8
CN	H	**1e**^{2}	$(-54.9)_1$	7.8	62.7	84.5	74.9 (76.3 ± 3.0)	36.9
		1e^1	$(-54.9)_1$	7.8	62.7	74.2	64.6	26.6
NO_2	H	**1f**^{2}	$(-19.1)_1$	34.8	53.9	82.3	99.7	61.7
		1f^1	$(-98.5)_3$	34.8	133.3	72.1	89.5	51.5
F	H	**1g**^{2}	$(-138.8)_2$	−2.2	136.6	92.0	72.4	34.4
		1g^1	$(-138.8)_2$	−2.2	136.6	90.6	71.0	33.0
NH_2	H	**1h**^{2}	$(-148.7)_4$	−23.7	125.0	88.1	47.0	9.0
		1h^1	$(-148.7)_4$	−23.7	125.0	81.0	39.9	1.9
OH	H	**1i**^{1}	$(-142.5)_3$	−13.3	129.2	88.7	58.0	20.0
		1i^2	$(-142.5)_3$	−13.3	129.2	87.9	57.2	19.2
CF_3	H	**1j**^{2}	$(-92.4)_2$	1.3	93.7	87.7	71.6	33.6
		1j^1	$(-92.4)_2$	1.3	93.7	80.7	64.6	26.6
F	CH_3	**1k**^{2}	$(-127.2)_2$	−7.6	119.5	92.7	67.6	29.6
		1k^1	$(-127.2)_2$	−7.6	119.5	89.8	64.8	26.8
CN	CH_3	**1l**^{2}	$(-64.8)_1$	1.22	66.0	85.2	69.1	31.1
		1l^1	$(-64.8)_1$	1.22	66.0	75.3	59.1	21.1
NO_2	CH_3	**1m**^{2}	$(-27.5)_1$	27.8	55.3	81.9	92.4	54.4
		1m^1	$(-102.5)_3$	27.8	130.3	70.2	80.6	42.6
CF_3	CH_3	**1n**^{2}	$(-98.3)_2$	−4.1	94.2	87.7	66.2	28.2
		1n^1	$(-98.3)_2$	−4.1	94.2	81.6	60.1	22.1
$H_2C^2{=}C^1{=}CH_2$		**2**^{1}	$(-104.3)_1$	−20.7	83.6	90.5	52.4 (50.5 ± 2.2)	14.4
		2^2	$(-104.3)_1$	−20.7	83.6	72.7	34.6	−3.4

[a] The sites of the H^- attack are denoted by superscripts 1 and 2 corresponding to carbon atom C^1 and C^2, respectively. Available experimental data given within parentheses are taken from ref 6. Indices below parentheses denote *n*th Koopmans' electron affinity.

between the B3LYP result (38 kcal mol^{-1}) and experiment (34.1 kcal mol^{-1}) for ethyne is 4 kcal mol^{-1}, which calls for careful scrutiny. Additional G2, G3, and G3(MP2) calculations give HAs of 34.3, 34.1, and 36.5 kcal mol^{-1}, respectively, implying that the G3 value is in perfect accordance with experiment (Table 2). It follows that the B3LYP computational procedure might be occasionally in error up to 4 kcal mol^{-1}. Hence, the B3LYP results should be taken with due care. The source of error of the adopted B3LYP scheme is in the first adiabatic electron affinity, which is by 4.4 kcal mol^{-1} too low. Koopmans' and the relaxation terms are higher by 2.1 and 6.5 kcal mol^{-1}, respectively. On the other hand, the bond association energy is smaller by a very small amount of 0.6 kcal mol^{-1}. Interestingly, the structural parameters computed by the 6-31+G(d,p) basis set including diffuse function did not significantly affect the B3LYP results.

Bearing this in mind, it is fair to conclude that the calculated HAs reproduce the trend of changes in a family of related molecules reasonably well, implying that the substituent effects are well described. It is, namely, plausible to assume that the relative values of HAs against the parent ethyne will partially cancel out the errors. This is of importance, because results can be used as approximate, but useful estimates of the HAs in cases where the measured data are not available.

Rationalization of the Trend of Changes of the Hydride Affinities. Let us focus on the interpretation of the results by trichotomy analysis, which are presented in Table 1. The first observation to be made is that all electron affinities $(EA)_n^{Koop}$ are negative, meaning that the electron is unbound in the frozen molecule picture. Further, the first adiabatic electron affinity $(EA)_1^{ad}$ is positive for ethyne substituted by CN, NO_2, and CF_3 groups, implying that their anions are quite stable species. In the case of the NO_2 group the excess electron is bound by a large $(EA)_1^{ad}$ value of 32.8 kcal mol^{-1}. Although the fixed electron density and clamped nuclei picture gives sometimes unphysical negative values for the electron capture, triadic analysis offers useful results in interpreting hydride ion affinities (HAs) within a series of related molecules. It provides a simple, approximate but useful rationalization of the trend of changes in substituted ethynes, which is in accordance with empirical knowledge and intuition. We would like to reiterate that the principal MO ensuring the most suitable accommodation of the excess electron is not always LUMO ($n = 1$). On the contrary, it is the second MO for F and CF_3 substituents and the third MO for H, CH_3, and OH atom or groups counting from LUMO as the first virtual molecular orbital (Figure 2). This is in line with our finding that HOMO is not always the best orbital either in trichotomy description of protonation of neutral and anionic bases.[17,18,20] The point is that the frontier HOMO and LUMO orbitals are not the most active molecular orbitals in very many cases of the protonation, deprotonation, and hydride addition[21] reactions, respectively, as it was amply illustrated earlier. In some cases, however, $n = 1$ as in **1e**, **1f**, **1l**, or **2**, meaning that PRIMOs coincide with the lowest unoccupied orbitals. The principal LUMO + *m* orbitals are pinpointed by a criterion that the corresponding excess electron density is adapted the best for creation of a new bond with the H atom. A useful hint is obtained by considering the optimized final structure of the hydride. Inspection of Figure 2 clearly shows for example that LUMO + 2 and LUMO + 3 in ethyne are degenerate due to symmetry and possess the electron density distribution sticking out of the symmetry axis, thus being well prepared for formation

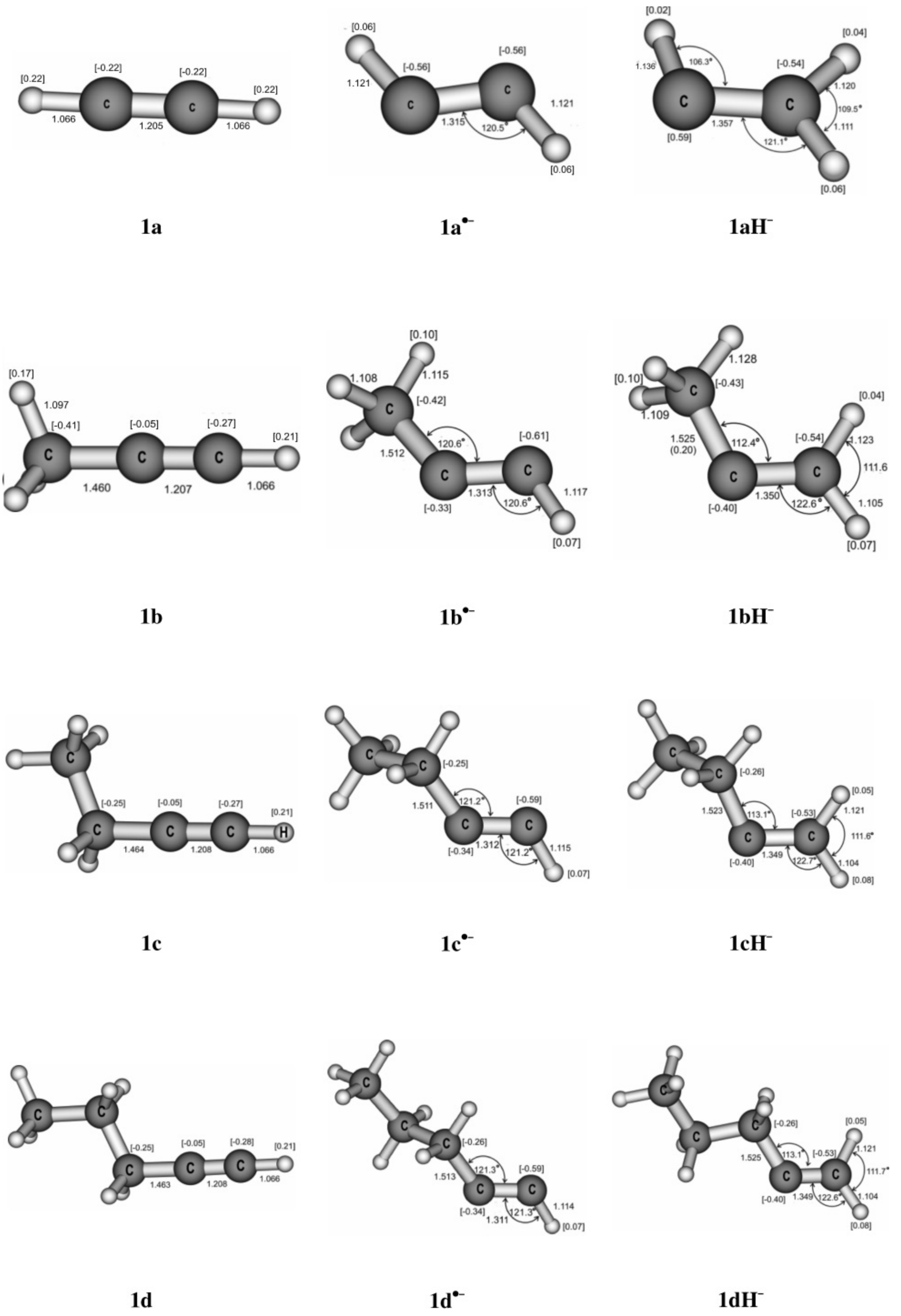

1a $\mathbf{1a^{\bullet-}}$ $\mathbf{1aH^-}$

1b $\mathbf{1b^{\bullet-}}$ $\mathbf{1bH^-}$

1c $\mathbf{1c^{\bullet-}}$ $\mathbf{1cH^-}$

1d $\mathbf{1d^{\bullet-}}$ $\mathbf{1dH^-}$

Figure 1. Part 1 of 3

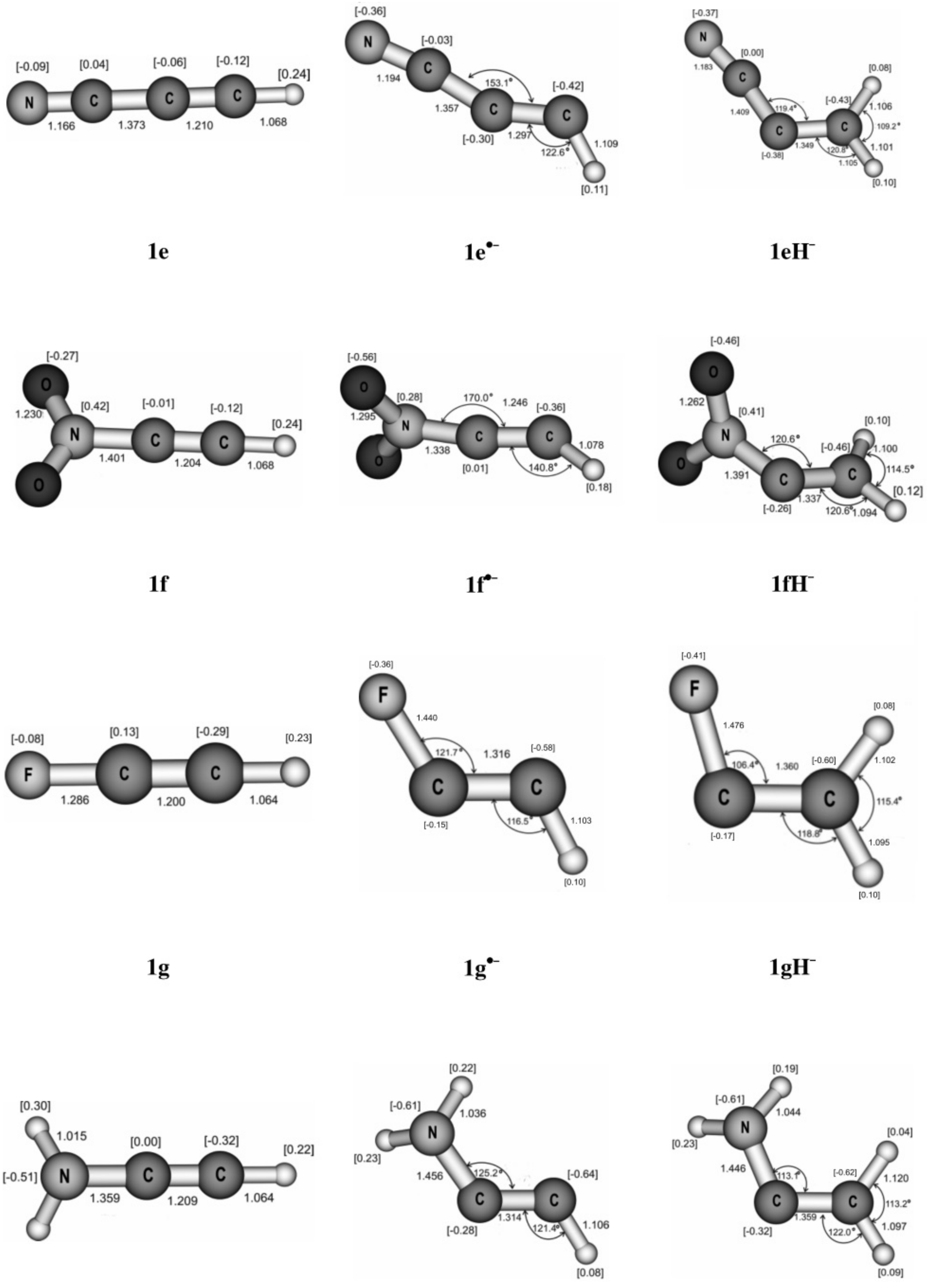

1e **1e$^{\bullet-}$** **1eH^{-}**

1f **1f$^{\bullet-}$** **1fH^{-}**

1g **1g$^{\bullet-}$** **1gH^{-}**

1h **1h$^{\bullet-}$** **1hH^{-}**

Figure 1. Part 2 of 3

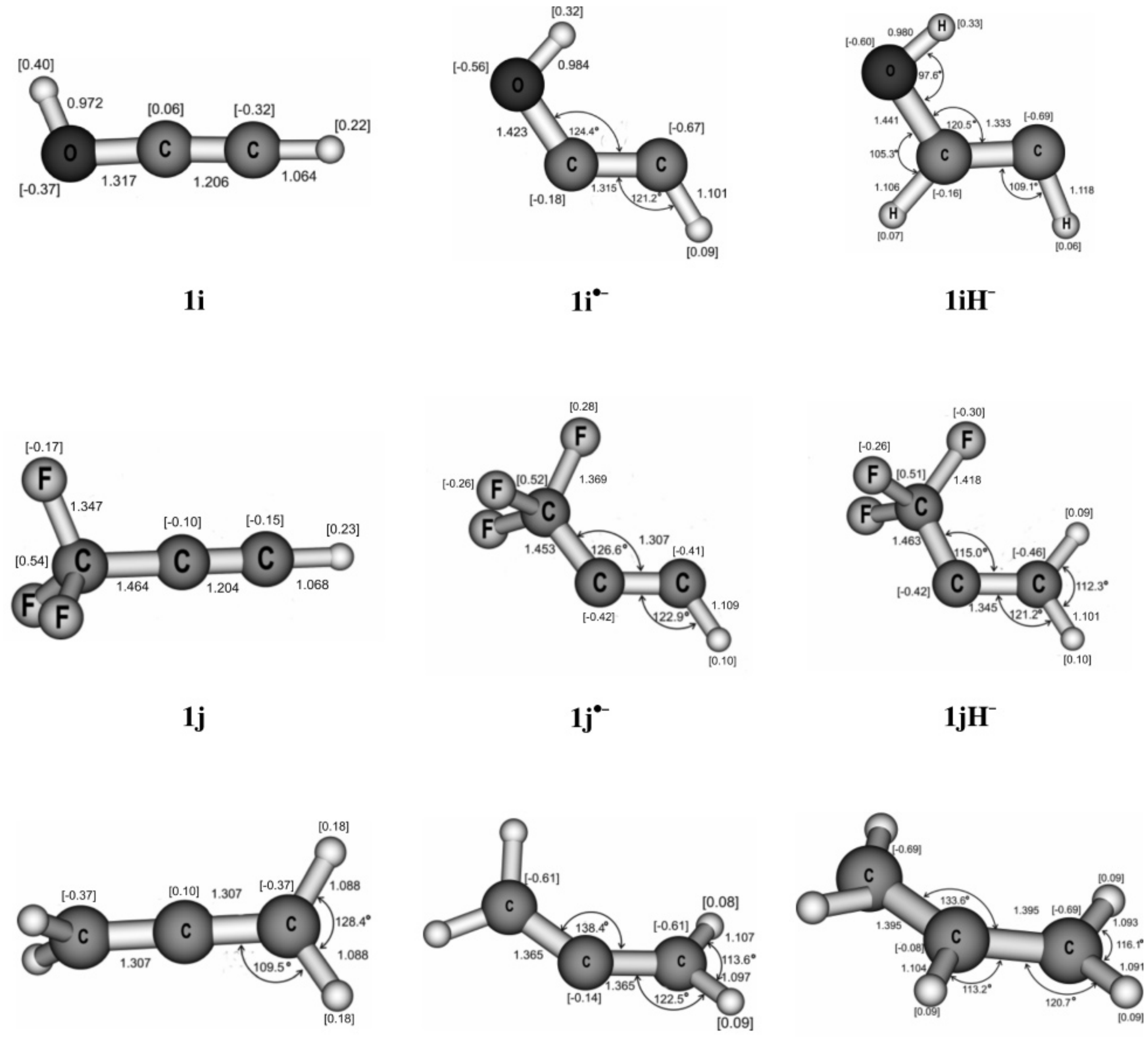

1i **$1i^{\bullet-}$** **$1iH^-$**

1j **$1j^{\bullet-}$** **$1jH^-$**

2 **$2^{\bullet-}$** **$2H^-$**

Figure 1. Part 3 of 3. Selected bond lengths obtained by the B3LYP/6-31G(d) method (in Å), π-bond orders (given within parentheses in |e|), and Löwdin atomic charges (in square brackets in |e|) for monosubstituted ethynes, their anions, and their hydrides.

of a new C−H bond. The same holds for LUMO + 1 and LUMO + 2 in fluoroethyne. The amino derivative **1h** does not have the axial symmetry, and consequently LUMO + 2 and LUMO + 3 are not equivalent. Both possess some π-type electron density at the unsubstituted carbon atom. However, it turns out that this density is higher in the LUMO + 3 orbital. Moreover, attachment of the H atom near the maximum electron density at the C^1 atom belonging to the LUMO + 3 orbital would lead most directly to the final **1hH**$^-$ geometry, after the appropriate rehybridization has taken place. Conseqently, the LUMO + 3 is the principal MO of choice. Selection of PRIMOs in **1i**, **1j**, **1k**, **1l**, **1m**, and **1n** can be made by inspection without any problem. It is interesting to notice that in the two disubstituted ethynes **1l** and **1m** the principal MOs are LUMO orbitals. In allene the LUMO orbital has high electron density at the central carbon atom. Hence, it is a suitable MO to accommodate the excess electron and to interact with the H atom. If follows that inspection of the virtual MOs gives a useful clue for the site of the H^- attack. It should be mentioned that the PRIMOs are the same for the hydride attack at both positions C^1 and C^2 as a rule. A notable exception is given by compounds **1f** and **1m** involving the NO_2 group. In both cases the H^- attachment at the most advantageous C^2 place includes LUMOs as the principal MOs. On the other hand, LUMO + 2 orbitals are PRIMOs for the hydride attack at the C^1 carbon atom.

The effect of substituents can be concisely described by selecting ethyne as a gauge molecule and taking a difference ΔHA relative to the parent gauge compound:

$$\Delta HA_\alpha = [\Delta(EA_n^{Koop}); \Delta(E(ea)^{(n)}_{rex}); \Delta(BAE)_\alpha^{\bullet-}] \quad (5)$$

where

$$\Delta(EA_n^{Koop}) = EA_n^{Koop}(\mathbf{M}) - EA_2^{Koop}(\mathbf{1a}) \quad (5a)$$

$$\Delta(E(ea)^{(n)}_{rex}) = E(ea)^{(n)}_{rex}(\mathbf{M}) - E(ea)^{(2)}_{rex}(\mathbf{1a}) \quad (5b)$$

$$\Delta(BAE)_\alpha^{\bullet-} = (BAE)_\alpha^{\bullet-}(\mathbf{M}) - (BAE)_1^{\bullet-}(\mathbf{1a}) \quad (5c)$$

and **M** stands for a molecule under study. It is also tacitly assumed that square brackets imply a summation of three terms.

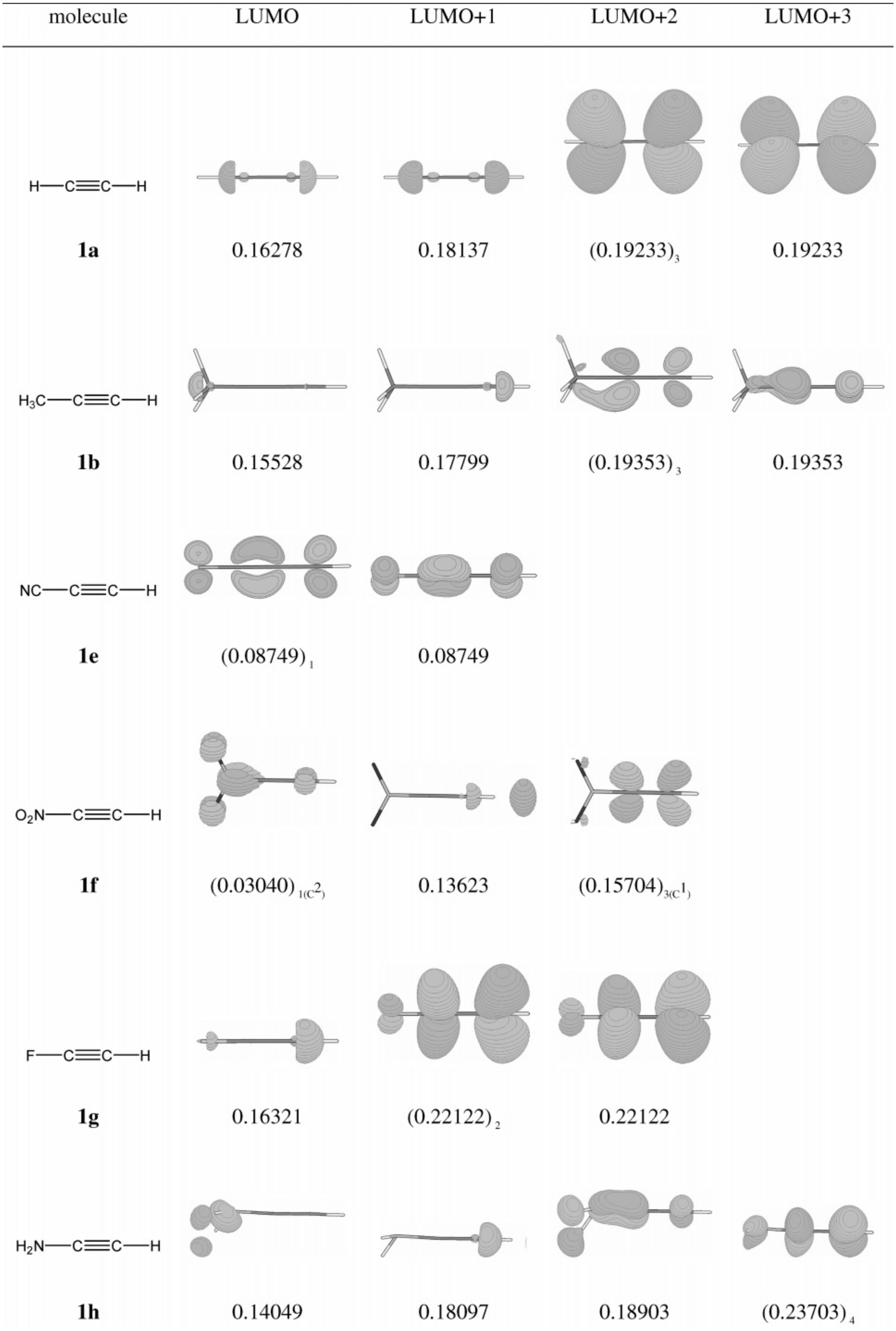

Figure 2. Part 1 of 2

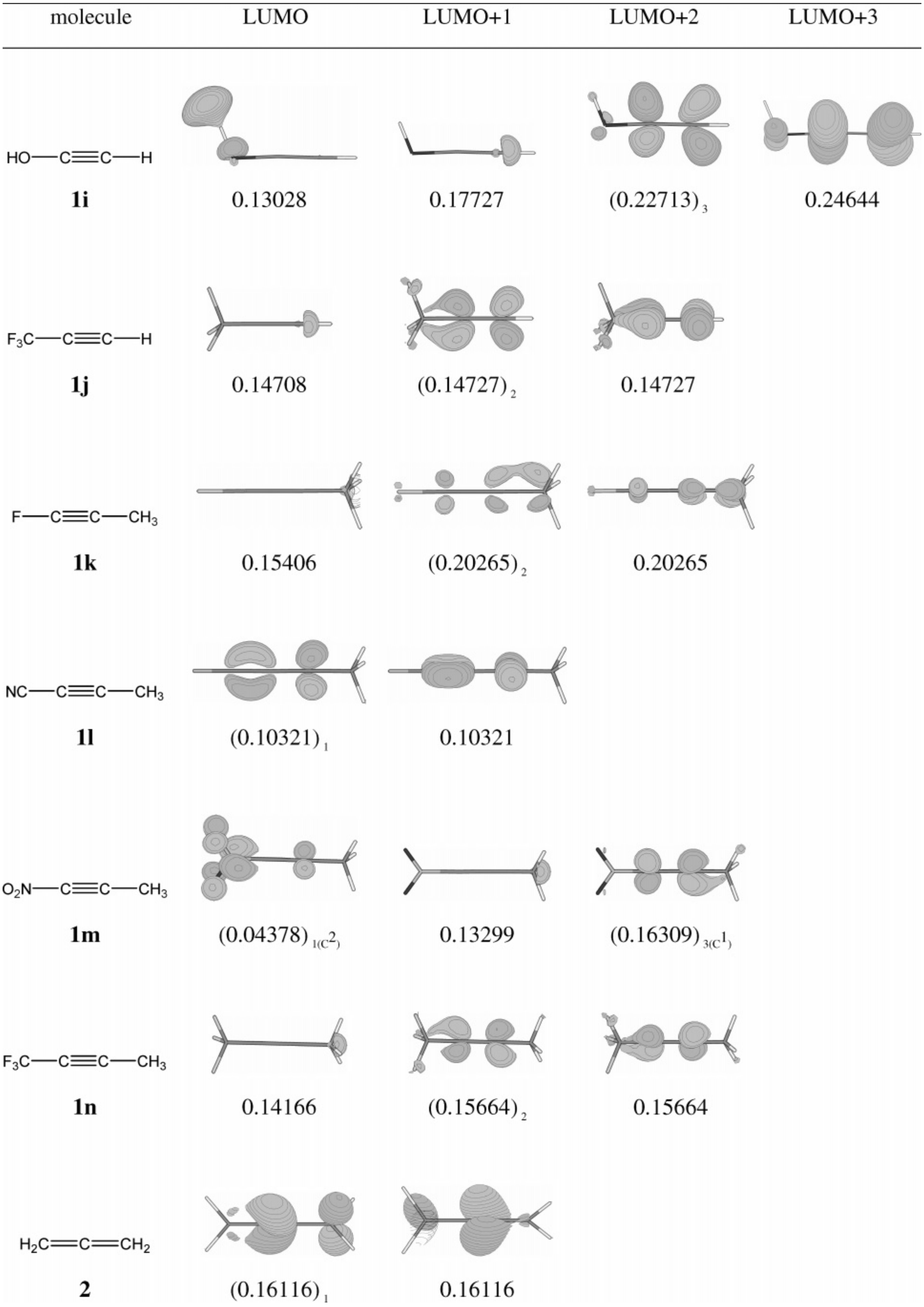

Figure 2. Part 2 of 2. Selected principal molecular orbitals obtained by the HF/6-311G(2d,p)//B3LYP/6-31G(d) model together with their orbital energies given within parentheses (in au). Indices below parentheses denote *n*th Koopmans' electron affinity. The former characterize the principal molecular orbitals. In cases where PRIMOs differ for different sites of the H$^-$ attack, they are additionally labeled by C^1 or C^2.

TABLE 2: Comparison of the Theoretical and Experimental Hydride Affinities for Ethyne and Their Resolution into Triadic Components (in kcal mol^{-1})[a]

model	$(EA)_n^{Koop}$	$(EA)_1^{ad}$	$E(ea)^{(n)}_{rex}$	$(BAE)^{\bullet -}$	HA(thr)
B3LYP/6-311+G(2df,p)//B3LYP/6-31G(d)	$-(120.7)_3$	−26.2	94.5	81.6	38.0
B3LYP/6-311+G(2df,p)//B3LYP/6-31G+(d,p)	$-(120.1)_3$	−25.6	94.5	81.3	38.2
G2	$-(118.7)_3$	−31.0	87.7	82.7	34.3
G3(MP2)	$-(118.6)_3$	−28.8	89.8	82.7	36.5
G3	$-(118.6)_3$	−30.6	88.0	82.2	34.1 [34.1]

[a] Experimental result given within square brackets is taken from ref 6.

Let us consider F, CN, CF$_3$, and NO$_2$ substituents first. A triad related to fluoroethyne **1g** reads [−18.1; 42.1; 10.4] = 34.4 (in kcal mol^{-1}), which means that the increased hydride affinity is a consequence of the favorable relaxation effect and stronger C−H bond energy given by the $(BAE)^{\bullet -}$ term. In contrast, Koopmans' term decreases the HA value of the **1g**. The corresponding triad for cyanoethyne **1e** is [65.8; −31.8; 2.9] = 36.9 (in kcal mol^{-1}), which shows an inverse picture. The enhanced hydride affinity takes place due to a "stabilization" of the LUMO orbital, which accommodates the excess electron. Here, "stabilization" should be conditionally understood, since the LUMO orbital energy is considerably lower relative to the LUMO + 2 orbital energy in **1a,** but it is still positive. The relaxation energy is significantly smaller in **1e**, whereas the bond association energy contributes only 3 kcal mol^{-1} to the hydride affinity amplification. It is interesting to note that the hydride affinities of **1g** and **1e** are close, although their origin is completely different. The triad describing the CF$_3$ effect in **1j** reads [28.3; −0.8; 6.1] = 33.6 kcal mol^{-1}, thus exhibiting qualitatively the same pattern as the cyano group. The notable difference is that Koopmans' and relaxation contributions are considerably smaller and larger, respectively, than in the **1e** case. It follows as a corollary that similar hydride affinities might result from completely different interplay of three terms. Finally, the extremal hydride affinity of nitroethyne **1f** can be predominantly ascribed to Koopmans' term, as evidenced by a triad [101.6; −40.6; 0.7] = 61.7 (in kcal mol^{-1}). It is a consequence of a dramatic lowering of the LUMO orbital energy whereas the relaxation term acts in the opposite direction. The methyl group in disubstituted ethynes **1k**, **1l**, **1m**, and **1n** diminishes the HA values by 4.8−7.3 kcal mol^{-1}. Particular terms within the triadic formula undergo substantial changes upon methylation as illustrated by triads for **1l** and **1m**, which take the form [55.9; −28.5; 3.6] = 31.1 kcal mol^{-1} and [93.2; −39.2; 0.3] = 54.4 kcal mol^{-1}, respectively. However, the general pattern remains the same.

An interesting finding is the fact that the H$^-$ attachment energies $(BAE)^{\bullet -}$ span a very narrow range of only 10 kcal mol^{-1} (82−92 kcal mol^{-1}), meaning that they are little dependent on the substituent on the other side of the molecule in monosubstituted derivatives. In same vein the $(BAE)^{\bullet -}$ term is not substantially affected by disubstitution.

It is important to realize that a difference in the hydride affinities between the C^1 and C^2 positions is given by a difference in the respective bond association energies, because in both cases the first adiabatic electron affinity $EA_1^{ad}(M) = EA_n^{Koop}(M)_\alpha + E(ea)^{(n)}_{rex}$ is the same, which holds in general. If PRIMOs are different for two positions in the same molecule, as in **1f** and **1m**, then $EA_n^{Koop}(M)$ and $E(ea)^{(n)}_{rex}$ are different, but their sum is invariant (viz. Table 1 and Figure 2).

In allene **2** the central carbon atom is most susceptible to the H$^-$ addition. The former compound is transformed to a planar allyl anion **2H$^-$** upon the H$^-$ attack, which exhibits a strong anionic resonance, as it is well-known. The origin of the HA value of 52.4 kcal mol^{-1} is given by a strong relaxation effect and an even higher stabilization provided by the bond association energy (Table 1). It is the latter effect which makes the C^1 reactive center more favorable than the C^2 one by 17.8 kcal mol^{-1}. The $(BAE)^{\bullet -}$ term includes the anionic resonance stabilization over the planar allylic system.

Structural Features. Ethyne becomes a planar molecule upon H$^-$ attachment (Figure 1) with both carbon atoms rehybridized to approximately sp^2 canonical hybridization implying that a double bond is formed and that a lone pair residing on the opposite $=$CH fragment is in the molecular plane. It is important to reiterate that H$^-$ attacks the unsubstituted carbon atom in monosubstituted ethynes as a rule. Moreover, the resulting hydrides are generally planar in order to ensure the optimal π-electron resonance effect. It is taken for granted here, that in the case of the CF$_3$ group the fluorine atoms are sticking out of the molecular plane in **1nH$^-$**, but its carbon atoms lie in the molecular plane. The H atoms of the NH$_2$ group are also not coplanar. They are shifted out of the molecular plane in such a way in **1h$^{\bullet -}$** and **1hH$^-$** that the lone pairs are situated in orthogonal planes. This conformation enables a resonance between the NH$_2$ group and the double bond. A very interesting nonplanarity is exhibited by the NO$_2$ group in the **1f** derivative. It is found, in both the anion radical **1f$^{\bullet -}$** and hydride **1fH$^-$**, that the NO$_2$ group assumes orientation which is perpendicular to the C$=$CH$_2$ plane, thus ensuring a resonance between the NO bonds and the π double bond. Another interesting conformational feature is a finding that the CH bonds in **1f$^{\bullet -}$** and **1fH$^-$** as well as the CF bonds in **1j$^{\bullet -}$** and **1jH$^-$** are placed in staggered positions relative to the lone pair of the nearest neighbor carbon atom.

Let us discuss bond distances of ethyne **1a**, its anion radical **1a$^{\bullet -}$**, and hydride **1a$^-$** in some more detail as calculated at different levels of theory (Figure 3). It is well-known that the HF model underestimates the bond distances of triple and double bonds. They are indeed larger when computed by the B3LYP and MP2 procedures, which in turn remedy this drawback of the HF model to a great deal. A survey of the presented data shows that the structural features predicted by the B3LYP/6-31G(d) method are in good agreement with those estimated by the MP2/6-31G(d) method (Figure 3). This lends credence to the computational scheme adopted in the present work. Introduction of the diffuse function in the B3LYP/6-31+G(d,p) scheme does not significantly affect the structural parameters. It is interesting that anions assume geometry which is very close in shape to that of the final products, hydrides. Thus, they are structurally well prepared for binding the H atom. We would like to underline that this is a general feature observed in all systems studied here (viz. Figure 1). Addition of the electron yielding **1a$^{\bullet -}$** radical anion leads to a bent S-like planar structure with two lone pairs in trans position. The CC and CH bonds are stretched by 0.11 and 0.06 Å relative to the neutral parent molecule. There are several reasons for these structural changes. The first is rehybridization of the carbon atoms, which will be

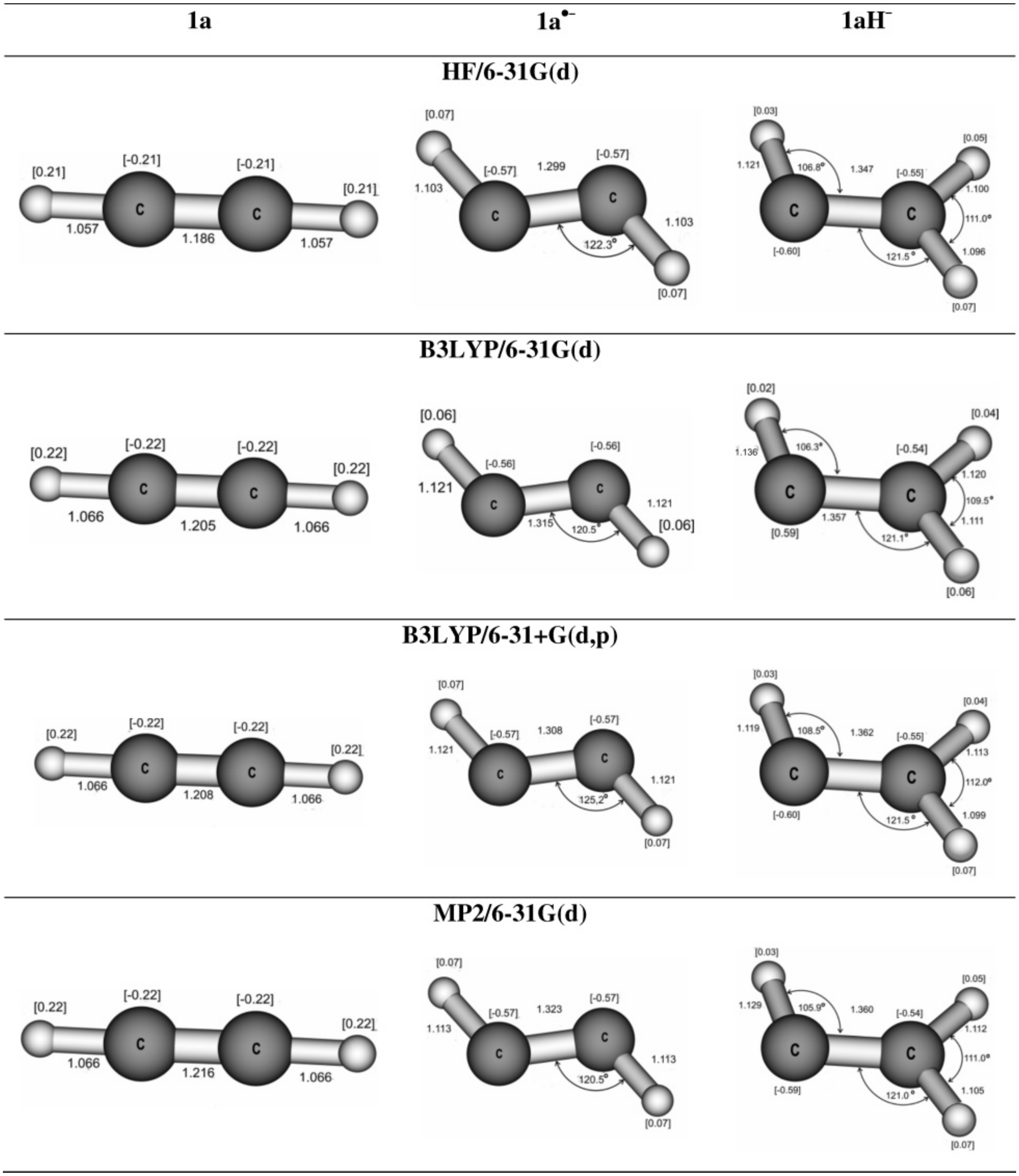

Figure 3. Selected bond lengths (in Å), and bond angles (in degrees) in ethyne, its anion, and its hydride calculated at different levels of theory.

discussed by using natural bond orbital s-character.[27] The latter are closely related to the bond distances and angles[28] as well as to many local properties associated with covalent bonding.[29] The average s-character (in percent) of the CC bond in ethyne of 52.0 drops to 45.3 in the **1a**$^{\bullet-}$ anion. A dramatic decrease in the s (%) character takes place for the CH bonds as evidenced by the 47.8% and 22.2% in **1a** and **1a**$^{\bullet-}$, respectively. The lone pairs assume s-character of 32.5%, i.e., by 10% higher than that of the CH bond. This is intuitively clear, because the lone pair prefers larger s-content in view of the lower energy of the s-orbital. The C^1 atom in the hydrided adduct **1aH**$^-$ undergoes a further rehybridization leading to a decrease in the s (%) for a hybrid participating in the CC σ-bonding adopting a value of 39.5%. The corresponding lone pair increases its s-character to 40%. A decrease in the s-character of hybrids forming covalent bond implies its lengthening.[28−30] Another useful index in discussing structural parameters is the π-bond order. We shall make use of the Löwdin symmetrical orthogonalization procedure[31] in considering partitioning of the electron density distribution into atomic and two-atom contributions. A brief comment on the choice of the atomic charges is in place here, because they are an important component of the interpretational schemes in chemistry. The first question is whether we have an experimental phenomenon which can be realistically described by the atomic monopoles (charges). In our opinion it is provided by the ESCA chemical shifts,[32] which in turn can be estimated to a good accuracy by the intramolecular electrostatic potential.[33] The latter is well reproduced by the atomic monopole approximation.[34] Unfortunately, many of the popular recipes of retrieving atomic charges from the MOs or total electronic densities are not appraised against ESCA shifts or simply by the calculation of the electrostatic potentials at the nuclei. This holds for stockholder[35] and QTAIM[16] charges too. This criterion is a severe test for e.g. the QTAIM charges, because they grossly exaggerate the intramolecular density drifts. In small molecules such as CO, H_2CO, and CH_3OH the oxygen gross atomic electron populations are as large as 9−9.5 electrons. This means that the electron density shift to oxygen is 1.0 to 1.5 |e|, which differs form all other methods.[36−39] It also implies that the CO bonds should be ionic in these compounds, which contradicts chemical experience. Additional difficulty inherent in the stockholder and QTAIM charges is the fact that the center of gravity of the electron density does not coincide with the atomic nuclei. Hence, higher multipoles have to be included in the electrostatic interactions.[25] Our choice of Löwdin atomic charges is prompted by the favorable feature that the problem of partitioning of the mixed densities is circumvented by symmetric orthogonalization. We do not pretend that it is the best way of defining atomic charges.

Going back to discussion of the structural parameters, it should be mentioned that a rather small CC distance in **1a**$^{\bullet-}$ (1.315 Å) is a consequence of a low Löwdin π-bond order (0.49 |e|) implying that the double π-bond is realized by only 50%. The CC bond is additionally lengthened by 0.04 Å due to a subsequent decrease in the s-character in **1aH**$^-$ as mentioned earlier. A distribution of Löwdin atomic charges is instructive. It appears that the electron density is increased at the C and H atoms by 0.34 and 0.16 |e| in the anion radical **1a**$^{\bullet-}$, implying that the excessive electron is distributed over all atoms, but the carbons are preferred by a factor of 2. Not unexpectedly, the atomic charges remain practically unchanged upon attachment of the neutral H atom yielding **1aH**$^-$. The changes in propyne **1b** follow the same pattern. The central C atom in **1b** and **1b**$^{\bullet-}$ has smaller electron density than the terminal carbons. This is understandable since it diminishes repulsion between the negatively charged terminal carbon atoms. This difference practically disappears in **1bH**$^-$, and the electron density distribution becomes almost even. It should be pointed out again that the excess electron is distributed overall the anions **1b**$^{\bullet-}$ and **1bH**$^-$. This is a general observation valid for all systems considered here. It is noteworthy that the carbon atom undergoing the H^- attachment contains more electron density than its counterpart possessing the lone pair. The rest of the data displayed in Figure 1 speak for themselves.

A point of considerable interest is that the H^- attack occurs at the unsubstituted carbon, which has significantly higher electron density than the substituted C atom. This finding suggests that the H^- attack is not so nucleophilic as one might expect, a conjecture which is valid for the Löwdin charges adopted in this work. Some more calculations with other types of atomic charges are necessary before the final conclusion can be drawn.

Concluding Remarks

The most important results of the present study are embodied in the calculated hydride affinities of substituted ethynes, which have not been submitted to experimental investigations so far. Theoretical HAs provide not only the most favorable sites of the H^- attack but also the energetic account for alternative positions. Additional information of equal importance is interpretation of the computed hydride affinities offered by triadic analysis. It is shown that similar HA values may result from completely different reasons. For instance, the increase in hydride affinity of fluoroethyne (34.4 kcal mol^{-1}) and cyanoethyne (36.9 kcal mol^{-1}) is a consequence of the dramatic increase in the relaxation energy and Koopmans' term, respectively. Further, it is found that the highest hydride affinities exhibit ethynes substituted by strong electronegative groups (NO_2 and CF_3) as intuitively expected. The H^- attachment at one of the carbons of the triple bond induces formation of the CC double bond, implying that the C atom, which is not attacked, possesses a lone pair. Finally, a salient structural feature of the hydrides is that substituent groups assume conformations which enable an optimal resonance effect with the CC double bond. Last but not least, the hydride affinities seem to provide a simple means of measuring the electrophilic propensity of compounds. This proposition should be better examined in the future.

Acknowledgment. We thank the Computing Centre of the University of Zagreb (SRCE) for granting computation time on the ISABELLA cluster.

References and Notes

(1) Smith, M. B.; March, J. *March's Advanced Organic Chemistry: Reactions, Mechanisms and Structure*, 5th ed.; John Wiley & Sons: New York, 2001.

(2) Cope, A. C.; Martin, M. M.; McKervey, M. A. *Q. Rev., Chem. Soc.* **1966**, *20*, 119.

(3) Carey, F. A.; Sundberg, R. J. *Advanced Ogranic Chemistry*, 4th ed.; Springer Sciences & Business Inc.: 2000; Part A, pp 316−323.

(4) Arnett, E. M.; Flowers, R. A.; Meekhof, A. E.; Miller, L. *J. Am. Chem. Soc.* **1993**, *115*, 12603.

(5) Arnett, E. M.; Flowers, R. A.; Ludwig, R. T.; Meekhof, A. E.; Walek, S. A. *J. Phys. Org. Chem.* **1997**, *10*, 499.

(6) Olah, G. A.; Molnar, A. *Hydrocarbon Chemistry*; Wiley-Interscience: New York, 1995.

(7) Lee, I.-S.; Chow, K.-H.; Kreevoy, M. M. *J. Am. Chem. Soc.* **2002**, *124*, 7755 and references therein.

(8) Frey, P. A. *FASEB J.* **1996**, *10*, 461.

(9) Cheng, J.-P.; Handoo, K. L.; Xue, J.; Parker, V. D. *J. Org. Chem.* **1993**, *58*, 5050.

(10) Handoo, K. L.; Cheng, J.-P.; Parker, V. D. *J. Am. Chem. Soc.* **1993**, *115*, 5067.

(11) Parker , V. D. *Acta Chem. Scand.* **1992**, *46*, 1133.

(12) Cheng, J.-P.; Handoo, K. L.; Parker, V. D. *J. Am. Chem. Soc.* **1993**, *115*, 2655.

(13) Hunter, E. P.; Lias, S. G. In *NIST Chemistry WebBook, NIST Standard Reference Database Number 69*; Mallard, W. G., Ed.; National Institute of Standards and Technology: Gaithersburg, MD, 2003. http://webbook.nist.gov.

(14) Mandado, M.; Van Alsenoy, Ch.; Mosquera, R. A. *Chem. Phys. Lett.* **2005**, *405*, 10 and references therein.

(15) Rosenberg, R. E. *J. Am. Chem. Soc.* **1995**, *117*, 10358.

(16) Bader, R. F. W. *Atoms in Molecules, A Quantum Theory*; Oxford University Press: Oxford, 1990.

(17) Maksić, Z. B.; Vianello, R. *J. Phys. Chem. A* **2002**, *106*, 419.

(18) Maksić, Z. B.; Vianello, R. *ChemPhysChem* **2002**, *3*, 696.

(19) Deakyne, C. A. *Int. J. Mass Spectrom.* **2003**, *227*, 601.

(20) (a) Vianello, R.; Maksić, Z. B. *J. Phys. Org. Chem.* **2005**, *18*, 699. (b) Vianello, R.; Maksić, Z. B. *Tetrahedron* **2006**, *62*, 3402. (c) Vianello, R.; Maskill, H.; Maksić, Z. B. *Eur. J. Org. Chem.* **2006**, 2581.

(21) Vianello, R.; Maksić, Z. B. *Inorg. Chem.* **2005**, *44*, 1095.

(22) Lias, S. G. Ionization Energy Evaluation. In *NIST Chemistry WebBook*, *NIST Standard Reference Database Number 69*; Linstrom, P. J., Mallard, W. G., Eds.; National Institute of Standards and Technology: Gaithersburg, MD, June 2005; 20899. http://webbook.nist.gov.

(23) Koopmans, T. *Physica* **1933**, *1*, 104.

(24) McGlynn, S. P.; Wittel, K.; Klasinc, L. In *Theoretical Models of Chemical Bonding, Part 3. Molecular Spectroscopy, Electronic Structure and Intramolecular Interactions*; Maksić, Z. B., Ed.; Springer-Verlag: Berlin-Heidelberg, 1991; p 99.

(25) C. J. Cramer, *Essentials of Computational Chemistry*, 2nd ed.; John Wiley & Sons: Chichester, 2004.

(26) Frisch, M. J.; Trucks, G. W.; Schlegel, H. B.; Scuseria, G. E.; Robb, M. A.; Cheeseman, J. R.; Zakrzewski, V. G.; Montgomery, J. A., Jr.;

Stratmann, R. E.; Burant, J. C.; Dapprich, S.; Millam, J. M.; Daniels, A. D.; Kudin, K. N.; Strain, M. C.; Farkas, O.; Tomasi, J.; Barone, V.; Cossi, M.; Cammi, R.; Mennucci, B.; Pomelli, C.; Adamo, C.; Clifford, S.; Ochterski, J.; Petersson, G. A.; Ayala, P. Y.; Cui, Q.; Morokuma, K.; Malick, D. K.; Rabuck, A. D.; Raghavachari, K.; Foresman, J. B.; Cioslowski, J.; Ortiz, J. V.; Baboul, A. G.; Stefanov, B. B.; Liu, G.; Liashenko, A.; Piskorz, P.; Komaromi, I.; Gomperts, R.; Martin, R. L.; Fox, D. J.; Keith, T.; Al-Laham, M. A.; Peng, C. Y.; Nanayakkara, A.; Gonzalez, C.; Challacombe, M.; Gill, P. M. W.; Johnson, B. G.; Chen, W.; Wong, M. W.; Andres, J. L.; Head-Gordon, M.; Replogle E. S.; Pople, J. A. *GAUSSIAN 98*, revision A.10; Gaussian, Inc.: Pittsburgh, PA, 1998.

(27) Foster, J. P.; Weinhold, F. *J. Am. Chem. Soc.* **1980**, *102*, 7211.

(28) Dewar, M. J. S.; Schmeising, H. N. *Tetrahedron* **1959**, *5*, 166.

(29) For review see: Maksić, Z. B. In *Theoretical Models of Chemical Bonding, Part 2, The concept of the Chemical Bond*; Maksić, Z. B., Ed.; Springer-Verlag: Berlin-Heidelberg, 1990; p 137.

(30) Kovačević, K.; Maksić, Z. B. *J. Org. Chem.* **1974**, *39*, 539.

(31) Löwdin, P. O. *J. Chem. Phys.* **1950**, *18*, 63.

(32) Siegbahn, K.; Nordling, C.; Johansson, G.; Hedman, J.; Haden, P. F.; Hamrin, K.; Gelius, U.; Bergmar, T.; Werme, L. O.; Manne, R.; Baer, Y. *ESCA Applied to Free Molecules*; North-Holland: Amsterdam, 1969 and references therein.

(33) Maksić, Z. B. In *Theoretical Models of Chemical Bonding, Part 3. Molecular Spectroscopy, Electronic Structure and Intramolecular Interactions*; Maksić, Z. B., Ed.; Springer-Verlag: Berlin-Heidelberg, 1991; p 289.

(34) Maksić, Z. B. Rupnik, K. *Z. Naturforsch.* **1983**, *38a*, 308.

(35) Hirshfeld, F. L. *Theor. Chim. Acta* **1977**, *44*, 129.

(36) Bader, R. F. W.; Bedall, P. M.; Preslak, J. *J. Chem. Phys.* **1973**, *58*, 557.

(37) Stutchbury, N. C. J.; Cooper, D. L. *J. Chem. Phys.* **1983**, *79*, 4967.

(38) Spackman, M. A.; Maslen, E. N. *J. Phys. Chem.* **1986**, *90*, 2020.

(39) Maslen, E. N.; Spackman, M. A. *Aust. J. Phys.* **1985**, *38*, 273.